ELSEVIER

Polymer 42 (2001) 8469–8475

polymer

www.elsevier.nl/locate/polymer

Side-chain intercrossing of poly(alkyl glutamate): LB and CP-MAS studies

Gunwoo Kim[a], Minseok Seo[a], Daewon Sohn[a,*], Duk-Young Han[b], Youngil Lee[c]

[a]*Department of Chemistry, Hanyang University, San 17, Haengdang-Dong, Sungdong-Ku, Seoul 133-791, South Korea*
[b]*Korea Basic Science Institute, Seoul Branch, Seoul, South Korea*
[c]*Dongbu Research Council, Daejeon, South Korea*

Received 4 December 2000; received in revised form 26 January 2001; accepted 31 January 2001

Abstract

The side-chain intercrossing of the substituted polyglutamate has been suspected as the main reason for the inhomogeneous monolayer at the air/water interface as well as the multi-domains in bulk. Before the side-chain melting at 60°C, the substituted chain intercrossing was confused by several experimental approaches. Here, we investigated the side-chain intercrossing of ethyl, hexyl, and stearyl substituted polyglutamate by surface pressure–surface area (π–A) isotherms and CP-MAS (cross-polarization magic angle spinning) NMR. We verify that the solvent drying process may be the main cause of the intercrossing of the side-chains in the glutamate polymers and provide the quantitative information about the intercrossing ratios for the side-chain polyglutamates. At room temperature, 60–90% of the total length of the side-chain intercrossed and the intercrossing ratios decreased at higher temperatures. © 2001 Published by Elsevier Science Ltd.

Keywords: Polyglutamate; Rod-like polymer; Side-chain intercrossing

1. Introduction

Synthetic polypeptide, particularly side-chain poly(glutamates) motivated extensive studies because of their liquid crystalline behavior and the α-helical conformation [1]. Side-chains of the polyglutamate were introduced to increase the solubility and to reduce the melting temperature of the hardly soluble rod-like liquid crystalline polymers [2,3]. These molecules are also good mimetic models of biopolymers and attractive candidates for various applications in photonics and electronics [4–6]. The different degree of ordering caused by the side-chain length creates the self-assembly of glutamate polymers in supramolecular structures [7–15]. The side-chains, however, have been suspected as origins of the inhomogeneous monolayer at the air/water interface and the multi-domains in the bulk state [16]. Previous X-ray studies of side-chain polyglutamate in bulk reported that alkyl substituents with the number of carbon atoms more than 10 interdigitate and crystallize, in which the crystallites are located between the layers [17]. When the number of carbon atoms is less than 10, side-chains remain in a liquid-like state and the backbone is aligned along the molecular axis [18]. Copolymers of short and long alkyl-substituted glutamates were introduced to exhibit intermediate properties and to apply for the practical applications [19,20]. However, the wide-angle X-ray diffraction studies in bulk with poly(stearyl glutamate)-*co*-poly(methyl glutamate) did not provide a precise quantitative degree of interdigitation [21,22].

Here, the temperature dependence of side-chain intercrossing was investigated by the thermally controlled Langmuir–Blodgett (LB) trough to deduce the quantitative information of the side-chain intercrossing. The ratio of the side-chain intercrossing for the short and the long side-chain polyglutamates was determined and the results were compared with previous X-ray studies [18]. The aim of this paper is to verify the driving force to make the intercrossed structure of the side-chains of rod-like polymers: the intercrossing of the side-chain is serious in the solvent drying process rather than the heating and cooling processes, which was verified by the CP-MAS (cross-polarization magic angle spinning) NMR technique [23–29].

2. Experimental

2.1. Materials

Poly(γ-stearyl α, L-glutamate)s, PSLGs, were synthesized

* Corresponding author. Tel.: +82-2-2290-0933; fax: +82-2-2299-0762.
E-mail address: dsohn@hanyang.ac.kr (D. Sohn).

0032-3861/01/$ - see front matter © 2001 Published by Elsevier Science Ltd.
PII: S0032-3861(01)00359-7

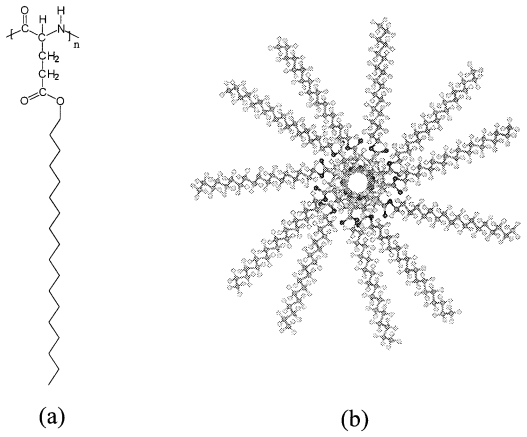

Fig. 1. (a) Chemical structure of PSLG and (b) its possible conformation (top view) for the 11 repeating units.

and provided by Prof. P.S. Russo at Louisiana State University [30]. The chemical structure of PSLG and its conformation (top view) are shown in Fig. 1.

We determined the number-average molecular weight to be 120,900, the weight-average molecular weight as 142,700, and the polydispersity as 1.18 for PSLG through gel permeation chromatography. Ethyl and hexyl substituted glutamate, referred to as PELG and PHLG were purchased from Sigma Chemical, and had M_w 48,700 and 60,500, respectively, as determined by intrinsic viscosity and light scattering experiments.

2.2. Sample preparation

The samples were dissolved in HPLC grade chloroform to make a stock solution and the concentration was adjusted to approximately 0.1–0.2 mg/ml. The solutions were sealed and stored in a refrigerator until use. To measure the π–A isotherm, the following successive additional procedure was performed. A certain volume of solution was spread at the air/water interface, the system was allowed to reach equilibrium, and then the surface pressure was read. This procedure was repeated for each addition of solution and the average surface density was calculated assuming no mass desorption to the subphase. The relative humidity in the box of the LB trough was maintained above 85% during the experimental process.

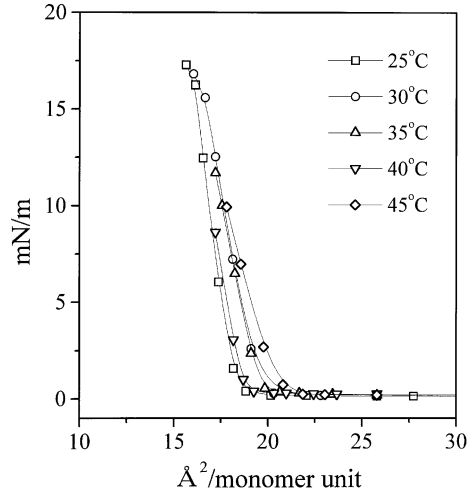

Fig. 2. Temperature dependence of π–A isotherm of 48.7k PELG. Temperatures are varied from 25 to 45°C.

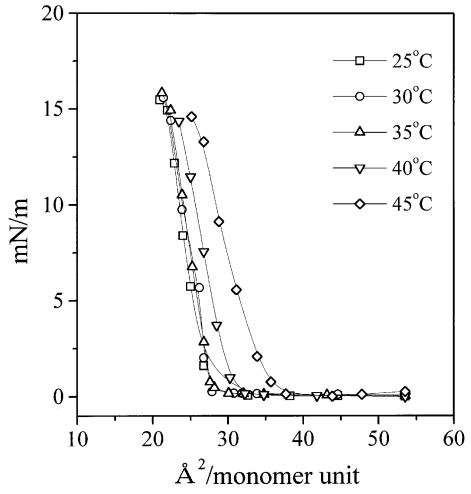

Fig. 3. Temperature dependence of π–A isotherm of 60.5k PHLG. Temperatures are varied from 25 to 45°C.

To measure the thickness of the monolayer, LB multilayer films were prepared on silicone wafer substrate by the routine process of Lauda FW2 LB trough. The wafers were cleaned in chloroform using an ultrasonicator for 20 min then further in a solution of $NH_4OH/H_2O_2/H_2O$ for 30 min. The wafers were rinsed with HNO_3 and then water to render their surface hydrophilic. The treated silicone wafers had a uniform surface with a root mean square roughness of 2 nm as determined by AFM.

2.3. Instruments

A Lauda FW2 LB trough was used to measure the π–A isotherm and the subphase temperature was controlled by a circulated water bath as mentioned previously in a paper [16]. The Rudolph automatic-nulling ellipsometer, Auto EL2, was used to measure the thickness of the multilayer of the LB film with operating wavelength, 632.8 nm, and angle of incidence, 70° ± 0.02. The experimental errors in the values of the phase difference (Δ) and azimuth (Ψ) were less than 0.03 and 0.02, respectively.

All 50.4 MHz ^{13}C NMR CP/MAS spectra were obtained on Varian unity Inova 200 solid-state NMR spectrometer in the temperature range of 30–80°C. Samples (ca. 100 mg) were contained in a zirconia rotor and spun at 2.5 kHz. The $\pi/4$ pulse length was 4.5 s. Contact time was 2.5 ms and delay time was 1.0 s. The spectral width and data points were 15 kHz and 2k, respectively. Spectra were accumulated 400 times. The ^{13}C chemical shifts were referenced

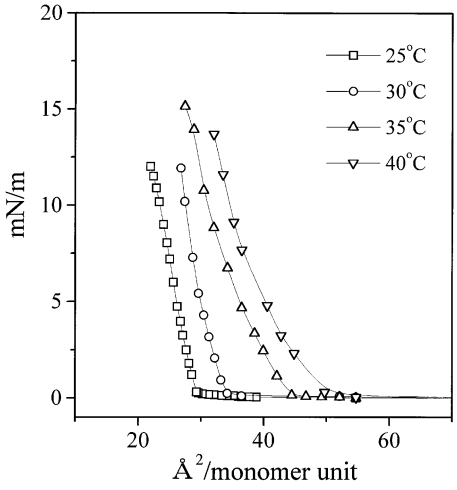

Fig. 4. Temperature dependence of π–A isotherm of 14.3k PSLG. Temperatures are varied from 25 to 45°C.

to hexamethylbenzene (HMB, 17.3 ppm) and converted to the values from TMS.

3. Results and discussion

Side-chain polyglutamates are generally believed that the helical backbone is laid down at the air/water interface and the side-chains are stretched out in the air [31]. At the same time, the crystalline side-chains intercross each other, but the helical backbones sustain their rigid structure at room temperature [32]. It was reported that the nematic monolayer at the air/water interface was formed during these processes [33]. The π–A isotherms represent stiff transition because of the rigid backbone, and the lift off points are around 20–30 Å^2/monomer depending on the side-chain length. In Figs. 2–4, the π–A isotherms of the different side-chain lengths of the polyglutamates as obtained using the successive additional method are displayed. The area per repeating unit at the monolayer state, A_0, is assigned by extrapolating the steep rise portion of the π–A isotherm to the x-axis. By increasing the temperature, the lift-off points (A_0) of the π–A isotherm shift to the large surface area, which indicates the large occupancy of a molecule at the air/water interface and a gradual lessening of the side-chain intercrossing with an increase in temperature. Fig. 2 shows the π–A isotherm of PELG at five different temperatures from 25 to 45°C. Increasing the subphase temperature from 25 to 45°C, the transition points of PELG shift from 18.35 to 20.69 Å^2/monomer and the slope is decreased. The shift of the π–A transition to higher areas with increasing temperature is a matter of thermal expansion of the monolayer. The thermal expansion of the monolayer deduces the side-chain intercrossing because these temperatures are below the side-chain melting and far below the denature of the α-helical conformation. Flexibility due to the loose side-chain intercrossing slightly lowers the slope of the π–A isotherm by increasing temperature as in Fig. 2.

Table 1
Calculated area/monomer (Å^2/monomer), diameter (Å), and side-chain length (Å) of PELG, PHLG, and PSLG by the π–A isotherms at different temperatures

		25°C	30°C	35°C	40°C	45°C
PELG	Area/monomer	18.35	19.54	19.56	20.23	20.69
	Diameter	12.23	13.03	13.04	13.49	13.79
	Side-chain length	3.32	3.71	3.72	3.95	4.10
PHLG	Area/monomer	27.19	27.86	27.89	30.53	34.95
	Diameter	18.13	18.58	18.60	20.36	23.31
	Side-chain length	6.27	6.49	6.50	7.38	8.85
PSLG	Area/monomer	29.13	33.42	43.18	47.05	
	Diameter	19.41	22.27	28.77	31.34	
	Side-chain length	6.91	8.31	11.58	12.87	

Previous molecular modeling and dynamic light scattering experiments suggest the molecular dimensions; the helical backbone has a pitch of 5.4 Å, and diameter of 5.6 Å with 3.6 monomer units in each revolution [21,22]. The average distance derived from the AM1 (Austin Model 1) semi-empirical calculation to the ethyl ester side-chains from the rigid backbone is 6.12 Å and corresponding area/monomer unit for the PELG is 26.76 Å^2/monomer, which is larger than the experimental value, 18.35 Å^2/monomer, deduced from the isotherm of PELG at 25°C. Based on these theoretical length of PELG, 6.12 Å, the side-chains intercrossing around 92% at 25°C was deduced. The experimental value at 45°C, 20.69 Å^2/monomer, is even smaller than the theoretical size of the molecule. The ratios of the side-chain intercrossing summarized in Table 1 are 78.8, 71.0, and 66.1% at 30, 40, and 45°C, respectively.

The π–A isotherms of hexyl (C = 6) substituted glutamate (PHLG) also shows stiff transition and shift to the larger surface area than that of PELG at increased temperatures as in Fig. 3. The lift-off points of the PHLG were 27.19, 27.89, 27.86, 30.53, and 34.95 Å^2/monomer at 25, 30, 35, 40, and 45°C, respectively. Based on the theoretical calculation of the fully extended chain of PHLG, 10.656 Å, the side-chains are 82.3% overlapped at 25°C. The π–A isotherms provide that the diameter of the PHLG is 18.13 Å and the side-chain length on one side is 6.27 Å.

The shift of the transition of PSLG (C = 18) was more dramatic than those of PELG and PHLG. Dynamic and static light scattering studies suggest the length and the diameter of 120k PSLG are 47.5 and 3.7 nm, respectively [30]. However, the diameter is much bigger than the value coming from the π–A isotherms, 1.94 nm, which indicates the side-chains are not fully extended at the air/water interface but are folded structures in the case of PSLG. The interlayer distance, from 1.1 to 2.5 nm, of PSLG in bulk was reported on the basis of X-ray data, which is similar to the size from the π–A isotherms and much smaller than the size of the PSLG in the solution [30]. Watanabe et al. reported the characteristic packing array of α-helices of C18 side-chains based on X-ray studies as the side-chains

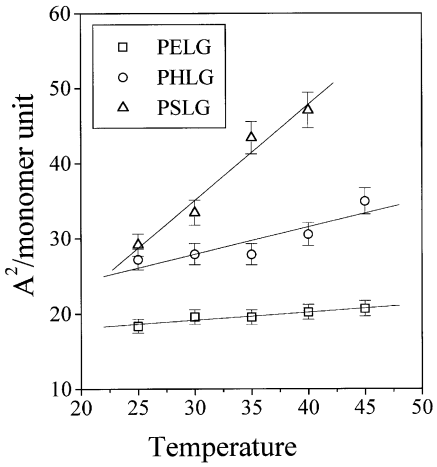

Fig. 5. Comparison of spacing between the poly(alkyl α, L-glutamate) by the π–A isotherms at different temperatures.

protruding from α-helices in neighboring layers intercalate with each other with their axes perpendicular to the layers [17]. They observed the side-chains passing through the unit area defined by the repeating length (27 Å) of the α-helix and the distance (12.3 Å) between molecules along the layer.

Fig. 5 summarizes the lift-off points of three polyglutamates at various temperatures. There are linear increments of transition points of PELG, PHLG, and PSLG by increasing the temperature. The transition point of PSLG at 25°C is only 2 Å^2/monomer unit above the transition of PHLG, but the increment of the surface area versus temperature, the gradient, is much bigger than that of PELG and PHLG. It is because the intercrossed ratio of PSLG is larger than that of PHLG and PELG. The spacing between the side-chains of PSLG was also measured by ellipsometry at two different temperatures, 25 and 35°C, as represented in Fig. 6. The LB film was prepared by dipping the silicon wafer vertically at the surface pressure, 5 mN/m. We have made five different LB films that consist of 2, 4, 6, 8, and 10 layers. The multi-layers were regularly increased and the average spacing between any two layers is 57.2 Å. The single layer thickness is 28.6 Å, which is bigger than the intermolecular distance of the PSLG at the air/water interface. The ellipsometry suggests that the degree of intercrossing of the upward side-chain is less than the sideward chains, which may come from the method of preparation of the monolayer. The sideward intercrossing was dominated by the instantaneous solvent evaporation, but the upward stacking was controlled by water evaporation after time intervals.

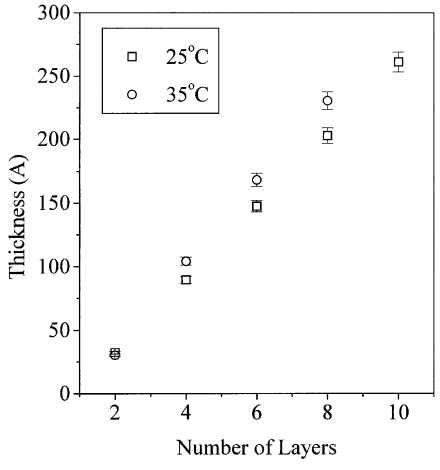

Fig. 6. Layer thickness of PSLG measured by an ellipsometry at two different temperatures.

Linear increments of the spacing at two different temperatures in the ellipsometry are observed in Fig. 6. The increment slope at 35°C is higher than that at 25°C, which means the side-chains are more expanded at the high temperature than the low temperature.

The intercrossing of the side-chains were constituted during the evaporation of the solvent ($CHCl_3$) at the air/water interface, and the solvent between the molecules evaporates fast at high temperature and the degree of intercrossing of the side-chains dwindles in the relatively high temperature subphase. These effects are more dramatic in the long side-chain PSLG. Instantaneous formation of the side-chain intercrossing of the glutamate polymer just after dropping the solution at the air/water interface was reported by several authors [34,35]. Epi-fluorescence images of PSLG at the air/water interface show multi-domains that indicate the interconnected structure of the side-chains [16]. The glutamate polymers are spread out in the constant temperature subphase. At high temperatures, the side-chains faced two driving forces: (1) the evaporation of the solvent which is the driving force to introduce the intercrossing of the side-chains by capillary forces, and (2) the thermal motion of the side-chains which releases the intercrossing of the side-chains. The capillary force between the side-chains due to the solvent evaporation is dominant at 25°C, but the thermal motions of the side-chains are raised by increasing the subphase temperature.

It is generally believed that the long side-chains maintain crystallinity below the side-chain melting temperature of 60°C [2,3]. However, we observed the sliding of neighboring side-chains, which were interlocked in PSLG. The structural changes of the side-chains before 60°C was not verified by previous IR spectra [36]. When we used the variable temperature FT-IR spectrophotometer, there is neither band shift nor intensity change over the temperature range of 25–60°C for the PELG and PHLG. The IR spectra of the PSLG between 25 and 80°C shows several vibrational bands change after 60°C, but there is no significant vibrational band change below 60°C. 60°C is the temperature of the endothermic transition of PSLG in differential scanning calorimeter (DSC). The variable temperature IR studies suggest that the conformational change of the side-chains occurs after the phase transition temperature, but the signals of the side-chain and rigid backbone are preserved below 60°C. Remaining question is what is the driving force to

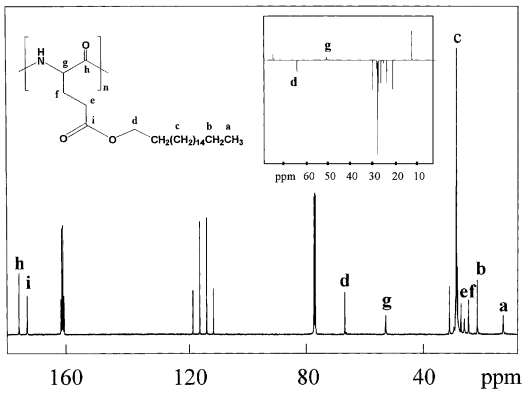

Fig. 7. ^{13}C NMR peak assignment. Inset is a spectrum of DEPT measurement of PSLG at 135° pulse, in which –CH– and $-CH_3$ show the positive values and $-CH_2$ shows the negative values.

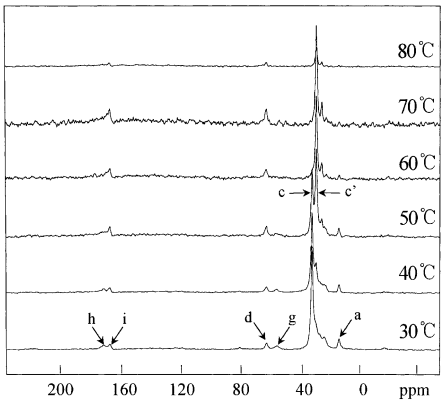

Fig. 8. CP-MAS NMR spectrum of PSLG after solvent drying. The assignment of each peak is in Table 2.

intercross and slide the side-chains at the air–water interface. CP-MAS NMR was used to investigate the motion on the side-chains of PSLG, a long side-chain polyglutamate. Fig. 7 indicates the assignment of each carbon atom of PSLG by ^{13}C NMR and the distortionless enhancement by polarization transfer (DEPT) technique. Most of the high intensity comes from the side-chain carbons, and the main chain carbon atoms produce very weak peaks but distinctive signals. Each peak is also assigned by the ACD software for the ^{13}C NMR.

Fig. 8 shows the temperature-dependent NMR spectra of 120k PSLG. The peak at 33.398 ppm indicates the alkyl side-chains and there is very little change in peak position and intensity before 60°C. We should remember that the temperature gradient IR spectra have the same trend.

However, when we carefully look at the NMR spectra, we can observe two split peaks at 34.27 and 31.31 ppm, as indicated c and c′ in Fig. 8 by increasing the temperature [37]. Fig. 9 shows the temperature-dependent ^{13}C NMR spectra of 120k PSLG after repeating a heating (to 80°C) and cooling (to 25°C) process, in which we can observe the distinct separation of the c and c′ peaks at relatively low temperature than Fig. 8.

Several carbon peaks (a, b, e, f, g, h) experienced dramatic changes by increasing the temperature. But ester CO (i) and $-OCH_2$ (d) do not change their peak intensity. The intensity of the carbons (a, b) at the end of the side-chain disappears by increasing the temperature from 30 to 80°C. The intensity of the carbons (f, e) at the β and γ positions sustained their intensity between 30 and 80°C, but the motion of the side-chain was detected by shifting of alkyl peak from 33.52 to 30.83 ppm (c to c′). It is known that 33.52 ppm is a chemical shift of *trans* zig-zag conformation in crystalline hydrocarbons (orthorhombic form) and 30.83 ppm is free rotating alkyls during increase of temperature [38]. The only difference between Figs. 8 and 9 is the process of the sample preparation. In Fig. 8, we prepared the sample by drying the solvent, chloroform, and directly measured the NMR spectrum. The side-chains might be intercrossed by the evaporation of the solvent and the evaporation energy exceeded the entropy compensation of the side-chain intercrossing. The tight array of side-chain crystals prevents the side-chain motion at 25–60°C. The thermal motions of the side-chains by increased temperature are interfered with the side-chain intercrossing. Through the measurement of the CP-MAS NMR spectrum after the heating–cooling process, two distinct features are observed.

First, the side-chain motions: we observed that the intensity of the peak at 33. 52 ppm was reduced, the peak at 30.83 ppm was sustained, and the peaks at 25.16 and 15.01 ppm disappeared, which indicates the deviation of the cross-polarization condition because of the side-chain motion. After passing the melting temperature, the zig-zag conformation and side-chain intercrossing are not recovered

Table 2
NMR peak assignment (ppm) of the PSLG at three different conditions: liquid state, solid state after drying the solvent, and solid state after heating and cooling process

	Ester (i)	Amide (h)	g	d	f	e	c	a
Liquid[a]	172.50	175.46	57.07	64.56	25.93	28.77	29.54	14.09
Solid 1[b]	172.42	176.64	57.78	64.73			33.52	14.94
Solid 2[c]	172.71	176.60	57.82	64.91			33.52 (30.83)	15.01

[a] $CDCl_3$ with 10% TFA solution NMR using 500 MHz Bruker AMX 500 by DEPT technique.
[b] Sample was prepared by drying the solvent.
[c] Obtained spectrum after heating and cooling process.

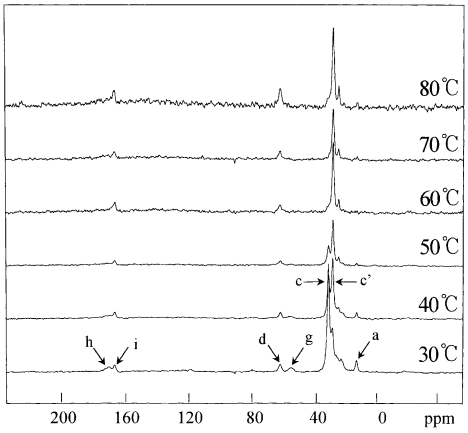

Fig. 9. CP-MAS NMR spectrum of PSLG after heating and cooling process. The assignment of each peak is in Table 2.

by the cooling process. That is the reason why the motions of the side-chains are distinctive in the CP-MAS NMR after repeating the heating and cooling processes.

Second, the main chain motions: the peaks at 53.44 and 175.88 ppm (g, h) also disappeared at increasing temperatures, which may be due to the distortion of the backbone. The proton-carbon cross-polarization technique uses the decoupling of the neighboring proton, so the disappearance of the carbon peaks at (g, h) may be due to the change of the original position of the backbone. It was reported that the rigid backbone structure of PSLG was maintained until 200°C and the liquid crystalline behavior was observed after 60°C through a polarized microscope [2,3]. Yamanobe et al. [39] also suggested that the motion of main chain by retaining the helical conformation. CP-MAS NMR only suggests the motion of the main chain, so we need more detail information based on IR spectroscopy and computer simulations.[1] Now, we can conclude that the distortion of the helicity of the peptide backbone starts at 40°C but the rod-like structure is sustained up to 200°C.

4. Concluding remarks

We have investigated the side-chain intercrossing and thermal behaviors for the series of poly(γ-alkyl α, L-glutamate). The side-chain and helix backbone preserved their crystallinity and rod-like structures between 25 and 60°C. We focused on the motions of the side-chains and conformations between 25 and 60°C because the interdigitations made multi-domains and their dynamic behaviors are unclear so far.

The intercrossed side-chains protruding from the neighboring molecules made monolayer at the air–water interface. And the degree of interdigitation of side-chains prevails in the solvent evaporation rather than the thermal annealing process. The degree of intercrossing of the side-chains can be determined by the π–A isotherm and it varied from 60 to 90% of the entire chain. The side-chains started to move by increasing the temperature and the motion is hindered by the geometry of the inter-crossed structure of the side-chains. The backbone structure was distorted due to the motion of long side-chains but the rod-like conformation was sustained during these whole processes.

[1] Another paper about the main chain motion based on IR spectroscopy and computer simulation is in preparation.

Acknowledgements

D.S. thanks Prof. P.S. Russo (Louisiana State University) for providing the PSLGs, and the Korea Basic Science Institute, Seoul Branch for allowing to use the NMR facilities. Authors gratefully acknowledge to Dr. Oc Hee Han at Korea Basic Science Institute, Daejeon for her valuable comments. This work was supported by a grant from KOSEF (981-0301-003-2).

References

[1] Block H. Poly(γ-benzyl-L-glutamate) and other glutamic acid containing polymers. New York: Gordon and Breach, 1983.
[2] Watanabe J, Takahina Y. Macromolecules 1991;24:3423.
[3] Tsujita Y, Ojika R, Tsuzuki K, Takizawa A, Kinoshita T. J Polym Sci, Part A: Polym Chem 1987;25:1047.
[4] Mathauer K, Mathy A, Bubeck C, Wegner G, Hickel W, Scheunemann U. Thin Solid Films 1992;210/211:449.
[5] Neher D. Adv Mater 1995;7:691.
[6] Mathauer K, Schmidt A, Knoll W, Wegner G. Macromolecules 1995;28:1224.
[7] Vierheller TR, Foster MD, Schmidt A, Mathauer K, Knoll W, Wegner W, Satija S, Majkrzak CF. Langmuir 1997;13:1712.
[8] Murthy NS, Samulski ET, Knox JR. Macromolecules 1986;19:941.
[9] Yan NX, Labes MM, Baek SG, Magda JJ. Macromolecules 1994;27:2784.
[10] Bu Z, Russo PS, Tipton DL, Negulescu II. Macromolecules 1994;27:6871.
[11] Tohyama K, Miller WG. Nature 1981;289:813.
[12] Kitaev V, Schillen K, Kumacheva EJ. Polym Sci: Polym Phys 1998;36:1193.
[13] Kitaev V, Kumacheva E. Langmuir 1998;14:5568.
[14] Muroga Y, Nagasawa M. Biopolymers 1998;45:281.
[15] Sohn D, Kitaev V, Kumacheva E. Langmuir 1999;15(5):1698.
[16] Sohn D, Yu H, Nakamatsu J, Russo PS, Daly WH. J Polym Sci, Part B: Polym Phys 1996;34(17):3025.
[17] Watanabe J, Ono H, Uematsu I, Abe A. Macromolecules 1985;18:2141.
[18] Tsujita Y, Ojika R, Takizawa A, Kinoshita TJ. Polym Sci, Part A: Polym Chem 1990;28:1341.
[19] Duda G, Schouten A, Arndt T, Lieser G, Schmidt GF, Bubeck C, Wegner G. Thin Solid Films 1988;159:221.
[20] Duda G, Wegner G. Macromol Chem, Rapid Commun 1988;9:495.
[21] Vierheller TR, Foster MD, Schmidt A, Mathauer K, Knoll W, Wegner G, Satija S, Majkrzak CF. Macromolecules 1994;27:6893.
[22] Mabuchi M, Ito S, Yamamoto M, Miyamoto T, Schmidt A, Knoll W. Macromolecules 1998;31:8802.
[23] Barendswaard W, Litvinov VM, Souren F, Scherrenberg RL, Gondard C, Colemonts C. Macromolecules 1999;32(1):167.
[24] Lopezcarrasquero F, Montserrat S, Deilarduya AM, Munozguerra S. Macromolecules 1995;28(16):5535.

[25] Thakur KAM, Kean RT, Zupfer JM, Buehler NU, Doscotch MA, Munson EJ. Macromolecules 1996;29(27):8844.
[26] Straus SK, Bremi T, Ernst RR. J Biomol NMR 1997;10(2): 119.
[27] Kricheldorf HR, Müller D. Macromolecules 1983;16(4):615.
[28] Zhao CH, Zhang HJ, Yamanobe T, Kuroki S, Ando I. Macromolecules 1999;32(10):3389.
[29] Cho G, Natansohn A, Ho T, Wynne KJ. Macromolecules 1996;29(7):2563.
[30] Poche DS, Daly WH, Russo PS. Macromolecules 1995;28: 6745.
[31] Schmidt A, Mathauer K, Reiter G, Foster MD, Stamm M, Wegner G, Knoll W. Langmuir 1994;10:3820.
[32] Riou SA, Chien BT, Hsu SL, Stidham HD. J Polym Sci, Part B: Polym Phys 1997;35(17):2843.
[33] Zental R. In: Stegemeyer, editor. Liquid crystals. New York: Steinkopff, 1994. p. 111 (chapter 3).
[34] Miyano K, Tamada K. Langmuir 1990;8:160.
[35] Miyano K, Tamada K. Langmuir 1993;9:508.
[36] Seo M, Jang K, Sohn D, Kang P, Choo J. Synth Met 2000;349: 155.
[37] Yamanobe T, Tsukahara M, Komoto T, Watanabe J, Ando I, Uematsu I, Deguchi K, Fujito T, Imanari M. Macromolecules 1988;21:48.
[38] VanderHart DL. J Magn Reson 1981;44:117.
[39] Yamanobe T, Tsukamoto H, Uematsu Y, Ando I, Uematsu I. J Mol Struct 1993;295:25.